Angiogenesis (2013) 16:29–44
DOI 10.1007/s10456-012-9297-6

ORIGINAL PAPER

Interleukin-8 reduces post-surgical lymphedema formation by promoting lymphatic vessel regeneration

Inho Choi · Yong Suk Lee · Hee Kyoung Chung · Dongwon Choi · Tatiana Ecoiffier · Ha Neul Lee · Kyu Eui Kim · Sunju Lee · Eun Kyung Park · Yong Sun Maeng · Nam Yun Kim · Robert D. Ladner · Nicos A. Petasis · Chester J. Koh · Lu Chen · Heinz-Josef Lenz · Young-Kwon Hong

Received: 7 March 2012 / Accepted: 16 August 2012 / Published online: 4 September 2012

Abstract Lymphedema is mainly caused by lymphatic obstruction and manifested as tissue swelling, often in the arms and legs. Lymphedema is one of the most common post-surgical complications in breast cancer patients and presents a painful and disfiguring chronic illness that has few treatment options. Here, we evaluated the therapeutic potential of interleukin (IL)-8 in lymphatic regeneration independent of its pro-inflammatory activity. We found that IL-8 promoted proliferation, tube formation, and migration of lymphatic endothelial cells (LECs) without activating the VEGF signaling. Additionally, IL-8 suppressed the major cell cycle inhibitor CDKN1C/p57^{KIP2} by downregulating its positive regulator PROX1, which is known as the master regulator of LEC-differentiation. Animal-based studies such as matrigel plug and cornea micropocket assays demonstrated potent efficacy of IL-8 in activating lymphangiogenesis in vivo. Moreover, we have generated a novel transgenic mouse model (K14-hIL8) that expresses human IL-8 in the skin and then crossed with lymphatic-specific fluorescent (Prox1-GFP) mouse. The resulting double transgenic mice showed that a stable

Electronic supplementary material The online version of this article (doi:10.1007/s10456-012-9297-6) contains supplementary material, which is available to authorized users.

I. Choi · Y. S. Lee · H. K. Chung · D. Choi · H. N. Lee · K. E. Kim · S. Lee · E. K. Park · Y. S. Maeng · N. Y. Kim · Y.-K. Hong (✉)
Department of Surgery, Norris Comprehensive Cancer Center, University of Southern California, 1450 Biggy St. NRT6501, Mail Code 9601, Los Angeles, CA 90033, USA
e-mail: young.hong@usc.edu

I. Choi · Y. S. Lee · H. K. Chung · D. Choi · H. N. Lee · K. E. Kim · S. Lee · E. K. Park · Y. S. Maeng · N. Y. Kim · Y.-K. Hong
Department of Biochemistry and Molecular Biology, Norris Comprehensive Cancer Center, University of Southern California, 1450 Biggy St. NRT6501, Mail Code 9601, Los Angeles, CA 90033, USA

I. Choi · Y. S. Lee · H. K. Chung · D. Choi · H. N. Lee · K. E. Kim · S. Lee · E. K. Park · Y. S. Maeng · N. Y. Kim · R. D. Ladner · N. A. Petasis · H.-J. Lenz · Y.-K. Hong
Norris Comprehensive Cancer Center, Keck School of Medicine, University of Southern California, Los Angeles, CA, USA

Present Address:
I. Choi
Department of Pharmaceutical Engineering, Hoseo University, Asan, Chungnam, Korea

T. Ecoiffier · L. Chen
Center of Eye Disease and Development, Program in Vision Science, and School of Optometry, University of California, Berkeley, CA, USA

R. D. Ladner
Department of Pathology, University of Southern California, Los Angeles, CA, USA

N. A. Petasis
Department of Chemistry, Dornsife College of Letters, Arts & Sciences, University of Southern California, Los Angeles, CA, USA

C. J. Koh
Division of Pediatric Urology, Children's Hospital Los Angeles and Keck School of Medicine, University of Southern California, Los Angeles, CA, USA

H.-J. Lenz
Division of Medical Oncology, University of Southern California, Los Angeles, CA, USA

expression of IL-8 could promote embryonic lymphangiogenesis. Moreover, an immunodeficient IL-8-expressing mouse line that was established by crossing K14-hIL8 mice with athymic nude mice displayed an enhanced tumor-associated lymphangiogenesis. Finally, when experimental lymphedema was introduced, K14-hIL8 mice showed an improved amelioration of lymphedema with an increased lymphatic regeneration. Together, we report that IL-8 can activate lymphangiogenesis in vitro and in vivo with a therapeutic efficacy in post-surgical lymphedema.

Keywords Lymphangiogenesis · Interleukin-8 · Prox1 · Lymphedema · Lymphatic endothelial cells

Introduction

The lymphatic system plays a major role in tissue fluid homeostasis by draining interstitial fluid, cells and macromolecules and transporting them back to the circulation [1]. Pathological tissue swelling, or lymphedema, occurs when the lymphatic system fails to function properly due to lymph node dissection, venous thrombosis or insufficiency, radiation, surgery and/or organ transplantation [2]. Lymphedema is one of the most common post-surgical complications among breast cancer survivals. Retrospective studies report that the incidence of lymphedema ranges from 5–10 % after lumpectomy alone, and up to 70 % after modified radical mastectomy, eventually affecting nearly 50 % of breast cancer survivors in the long run [3–9]. Although recent practice of sentinel lymph node biopsy tends to reduce such prevalence, this disfiguring and painful post-operative secondary lymphedema still remains a considerable physical and social burden to patients with very limited treatment options.

Molecular regulation of new lymphatic vessel formation, or lymphangiogenesis, has been a topic of intensive study in the past decade and, as a result, a number of essential molecules for lymphangiogenesis have been identified and characterized, including vascular endothelial growth factor (VEGF)-C, VEGF-D and VEGF receptor (VEGFR)-3 [10]. Moreover, VEGF-A, once thought to only control blood vessel growth [11], has been demonstrated to induce lymphatic vessel growth and sprouting as well [12–14], suggesting a conservation of common stimulatory pathways in both vascular systems. Similarly, fibroblast growth factor (FGF)-2, platelet-derived growth factor (PDGF), insulin-like growth factors (IGF-1/2), hepatocyte growth factor (HGF) and growth hormone (GH), were shown to activate both angiogenesis and lymphangiogenesis [15–20]. In addition to these growth factors, pro-inflammatory cytokines have been demonstrated to promote angiogenesis and lymphangiogenesis. Among them, interleukin (IL)-8 has been reported to activate chemotactic migration, proliferation and survival of vascular endothelial cells, and induce the expressions of VEGF and VEGF receptor [21–24]. Because IL-8 has been postulated to indirectly stimulate lymphangiogenesis through inflammation, its direct role in lymphangiogenesis has not been reported to date. In this study, we evaluated the therapeutic potential of IL-8 in lymphatic regeneration using various models and identified a direct effect of IL8 on in vitro and in vivo lymphangiogenesis.

Results

Expression of IL-8 and its receptor CXCR1 and CXCR2 in primary human lymphatic endothelial cells

Although the expression of CXCR1 and CXCR2 in blood vascular endothelial cells has been documented [25, 26], their expression in lymphatic endothelial cells (LECs) remain poorly characterized. Immunofluorescence analyses showed that CXCR2 is abundantly expressed in primary LECs, whereas CXCR1 is expressed at a low level, if any (Fig. 1a). Two receptors were found to be marginally upregulated in LECs after 6 h of treatment with a pro-inflammatory cytokine tumor necrosis factor (TNF)-α (1 ng/ml) (Fig. 1b). Notably, treatment of LECs with a higher dose (10 ng/ml) of TNF-α accelerated the expression of the two receptors; their upregulation was detectable within 2 h of treatment. On the other hand, IL-8 expression was detected in LECs without stimulation, and was upregulated 2-fold within 1 h of TNF-α treatment. Intensity of each PCR band was quantified and IL-8 expression was verified by quantitative real-time RT-PCR (qRT-PCR) (Supplemental Figure 1). In addition, 9-cis retinoic acid (9-cisRA), which we have recently identified as a novel pro-lymphangiogenic compound [27], was found to upregulate the expression of IL-8 mRNA in primary LECs 6 h post treatment (Fig. 1c, Supplemental Figure 1). The increased expression and secretion of IL-8 protein by 9-cisRA was detected by IL-8 ELISA assay (Fig. 1d). Together, our results demonstrate the prominent expression of IL-8 and its receptor in LECs, as well as their regulation by various stimuli such as TNF-α and 9-cisRA.

IL-8 promotes proliferation, tube formation and migration of primary human LECs

We next investigated the effects of IL-8 on proliferation, tube formation, and migration of LECs. IL-8 strongly promoted proliferation of LECs, which could be inhibited by an anti-IL-8 neutralizing antibody and a

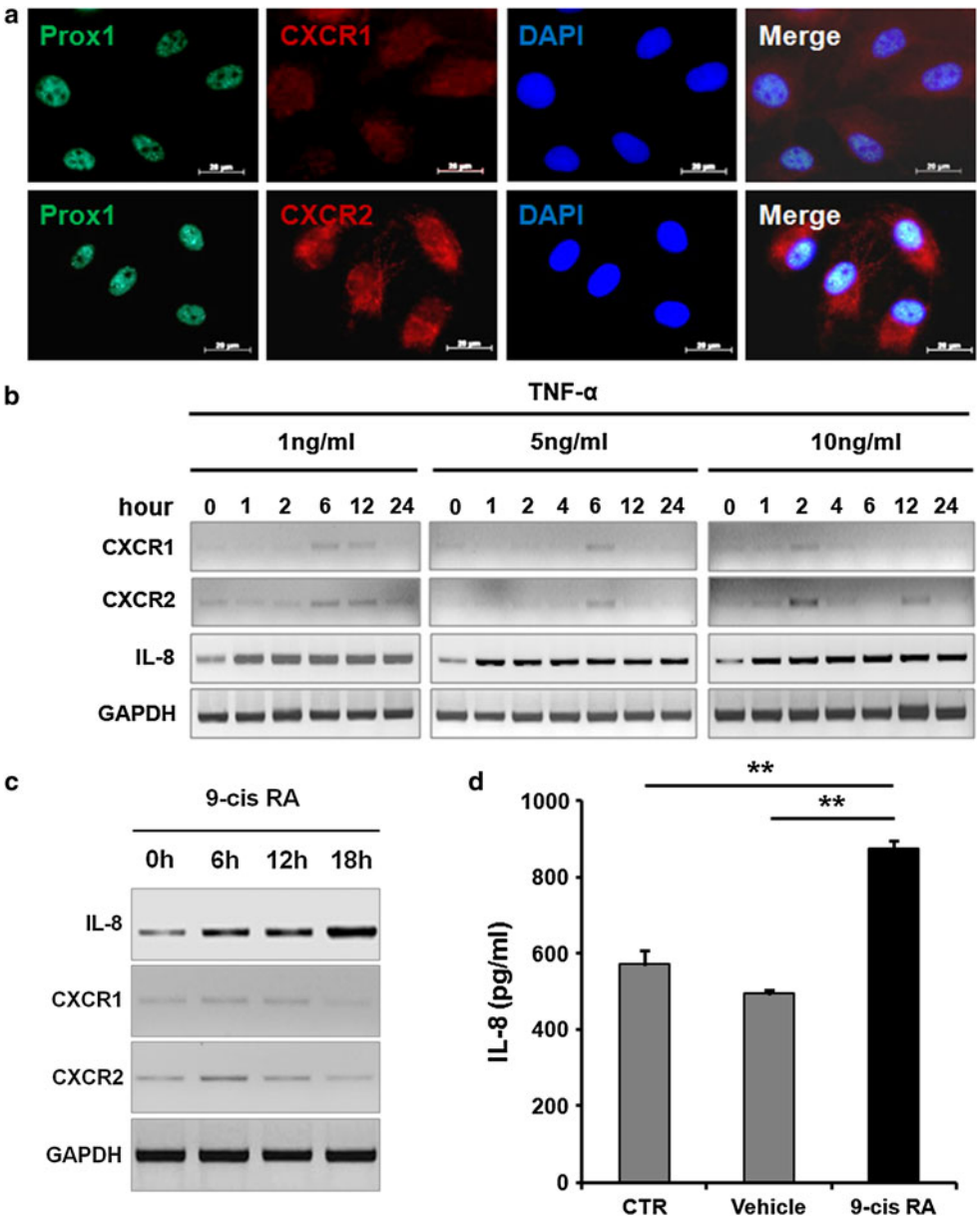

Fig. 1 IL-8 and CXCR2 are prominently expressed in LECs and regulated by TNF-α and 9-cis retinoic acid. **a** Immunofluorescent staining detecting the expression of CXCR1 and CXCR2, along with PROX1, on human primary dermal LECs. Nuclei and merged images are also shown. **b** Primary LECs treated with different dosages of TNF-α were analyzed for expression of IL-8 and it receptors by semi-quantitative conventional RT-PCR. Band intensities were quantified and shown (Supplemental Figure 1). Glyceraldehyde 3-phosphate dehydrogenase (GAPDH) was detected as an internal control. **c** Semi-quantitative conventional RT-PCR data show that IL-8 and it receptors were upregulated in primary LECs by 9-cisRA (1 μM). IL-8 expression was also determined by quantitative real-time RT-PCR (Supplemental Figure 1). **d** ELISA showing increased IL-8 secretion by LECs after treatment with 9-cisRA (1 μM) for 24 h. PCR-analyses were performed three times. Data shown as an average ± standard deviation. ** $p < 0.01$

CXCR2-specific chemical inhibitor SB225002 [28] (Fig. 2a). Because IL-8 was reported to induce proliferation of blood vascular endothelial cells by activation of VEGF signaling [24], we investigated the possible role of VEGF signaling in IL-8-induced LEC proliferation using chemical inhibitors (Ki8751 [29] and MAZ51 [30]) for VEGF receptors. While both chemical inhibitors suppressed VEGF-C-induced LECs proliferation, neither reagent showed any inhibition of IL-8-induced LEC proliferation, indicating that VEGF signaling does not play a role in IL-8-activated LEC-proliferation.

We next investigated whether IL-8 can promote tube formation of primary LECs and found that IL-8 enhanced the tube forming capability of LECs as potently as VEGF-C (Fig. 2b). Effect of IL-8 on non-directional migration of LECs was also studied using scratch assays performed on LEC monolayer that was either pre-treated with IL-8 or left untreated. After 18 h, the scratched area recovered more rapidly in IL-8-treated LECs compared to mock (vehicle)–treated LECs, and the IL-8-enhanced recovery was abrogated in the presence of a CXCR2 inhibitor SB225002 [28] (Fig. 2c). Together, this demonstrates that IL-8 significantly promotes the migration of LECs specifically through CXCR2. We then evaluated the IL-8-driven chemotactic effect on LECs using the modified Boyden chamber and found that IL-8 strongly activated directional migration of LECs (Fig. 2d). This IL-8-induced chemotactic activity of LEC could be blocked by a CXCR2 inhibitor SB225002,

but not by VEGFR inhibitors (Ki8751 [29] or MAZ51 [30]) that strongly inhibited VEGF-C-induced migration. Together, these in vitro lymphangiogenesis assays demonstrate that IL-8 can directly promote proliferation, tube formation, and migration of cultured primary human LECs through its receptor CXCR2.

IL-8 suppresses $p57^{Kip2}$ by downregulating its positive regulator PROX1

To study the molecular mechanism underlying IL-8-activated lymphangiogenesis, we analyzed the expression of PROX1, a master regulator of lymphatic development, since the regulation of PROX1 has been associated with LEC-proliferation [27, 31]. Notably, PROX1 expression was downregulated by IL-8 after 6 h and largely recovered by 24 h (Fig. 3a, Supplemental Figure 2). Moreover, because PROX1 acts as a positive regulator of the major cell cycle inhibitor $p57^{Kip2}$ by directly binding to its promoter in LECs [27], we evaluated the expression of $p57^{Kip2}$ upon IL-8 treatment, and found that IL-8 treatment resulted in downregulation of $p57^{Kip2}$ in LECs by 18 h. The expression of COUP-TFII, which interacts with PROX1 to regulate LEC differentiation [32], was not regulated by IL-8.

Our previous study demonstrated that 9-cisRA-induced LEC-proliferation by downregulation of $p57^{Kip2}$ expression, which was associated with removal of PROX1 protein from the $p57^{Kip2}$ promoter [27]. Since IL-8 reduces $p57^{Kip2}$ expression in LECs, we asked whether IL-8 causes a rapid dissociation of PROX1 protein from the $p57^{Kip2}$ promoter. Chromatin immunoprecipitation (ChIP) assays revealed that the PROX1 protein occupancy in the $p57^{Kip2}$ promoter was not affected by IL-8 treatment (Fig. 3b), suggesting that IL-8 and retinoic acids may utilize different mechanisms in downregulating $p57^{Kip2}$ expression. In order to investigate whether PROX1 mediates the IL-8-induced downregulation of $p57^{Kip2}$, we ectopically expressed PROX1 in LECs prior to IL-8 treatment. Indeed, the expression of $p57^{Kip2}$ was no longer suppressed by IL-8 in the presence of ectopic expression of PROX1 (Fig. 3c), indicating that PROX1 indeed mediates the downregulation of $p57^{Kip2}$ by IL-8. Moreover, knockdown of PROX1 in LECs using siRNA significantly increased IL8-expression based on qRT-PCR (Fig. 3d). Conversely, adenoviral expression of PROX1 resulted in IL-8 downregulation in blood vascular endothelial cells, where PROX1 is not expressed (Fig. 3e). Taken together, these data indicate that PROX1 mediates IL-8-induced downregulation of $p57^{Kip2}$, and that IL-8 and PROX1 reciprocally repress the expression of the other in LECs.

IL-8 activates in vivo lymphangiogenesis

We next evaluated the effect of IL-8 on lymphangiogenic in vivo using matrigel plug and cornea micropocket assays. For the matrigel plug assay, we took advantage of our lymphatic-specific fluorescent transgenic mice (Prox1-GFP) [33] to directly visualize lymphatic vessels with green fluorescence. We subcutaneously injected growth factor-depleted matrigel containing IL-8 or control matrigel into the lymphatic-specific GFP mice. After 2 weeks, matrigel plugs were harvested and the lymphatic vessel ingrowth was directly visualized. Indeed, the IL-8-containing matrigel plugs, but not control matrigel plugs, showed a prominent ingrowth of GFP-positive lymphatic vessels (Fig. 4a, Supplemental Figure 3). Moreover, the promotion of in vivo lymphangiogenesis by IL-8 was also assessed using mouse cornea micropocket assay. A slow-release pellet containing IL-8 or control pellet was implanted into mouse cornea, and, after 14-days, newly formed lymphatic vessels were quantified by immunofluorescent staining for a lymphatic marker LYVE-1 (Fig. 4b). This assay demonstrates that IL-8-releasing pellets could induce more pronounced lymphatic vessel growth compared to the control pellets (Fig. 4c). Taken together, both of the animal-based vascular assays consistently demonstrate that IL-8 strongly activates lymphangiogenesis in vivo.

Generation of transgenic mice expressing human IL-8 in the skin

We next generated a transgenic mouse line that expresses human IL-8 under the control of the keratin-14 (K14) promoter in order to establish an animal model that constantly secretes human IL-8 into the circulation (Fig. 5a). Because the K14-promoter is active selectively in keratinocytes in the basal epidermis layer of the skin [34], human IL-8 is expected to be produced from the basal keratinocytes and released into the system. Three founder lines expressing IL-8 at a concentration of 100–200 pg/ml in their serum were identified based on genotyping and ELISA (Fig. 5b,c). Moreover, the expression and secretion of human IL-8 from the keratinocytes was confirmed by immunohistochemistry (IHC) analyses on the skin section of wild-type and K14-hIL8 mice (Fig. 5d), establishing a novel skin-specific IL-8-expressing transgenic mouse line. Notably, it is believed that an IL-8 homologue does not exist in mouse and its functions were replaced by other chemokines such as Gro-α/CXCL1 and Gro-β/CXCL2 [35–37], all of which commonly bind to Cxcr2 [38]. Moreover, since human IL-8 has been found to be a poor agonist for mouse Cxcr2 [36], we wanted to confirm the functionality of human IL-8 secreted by the skin of

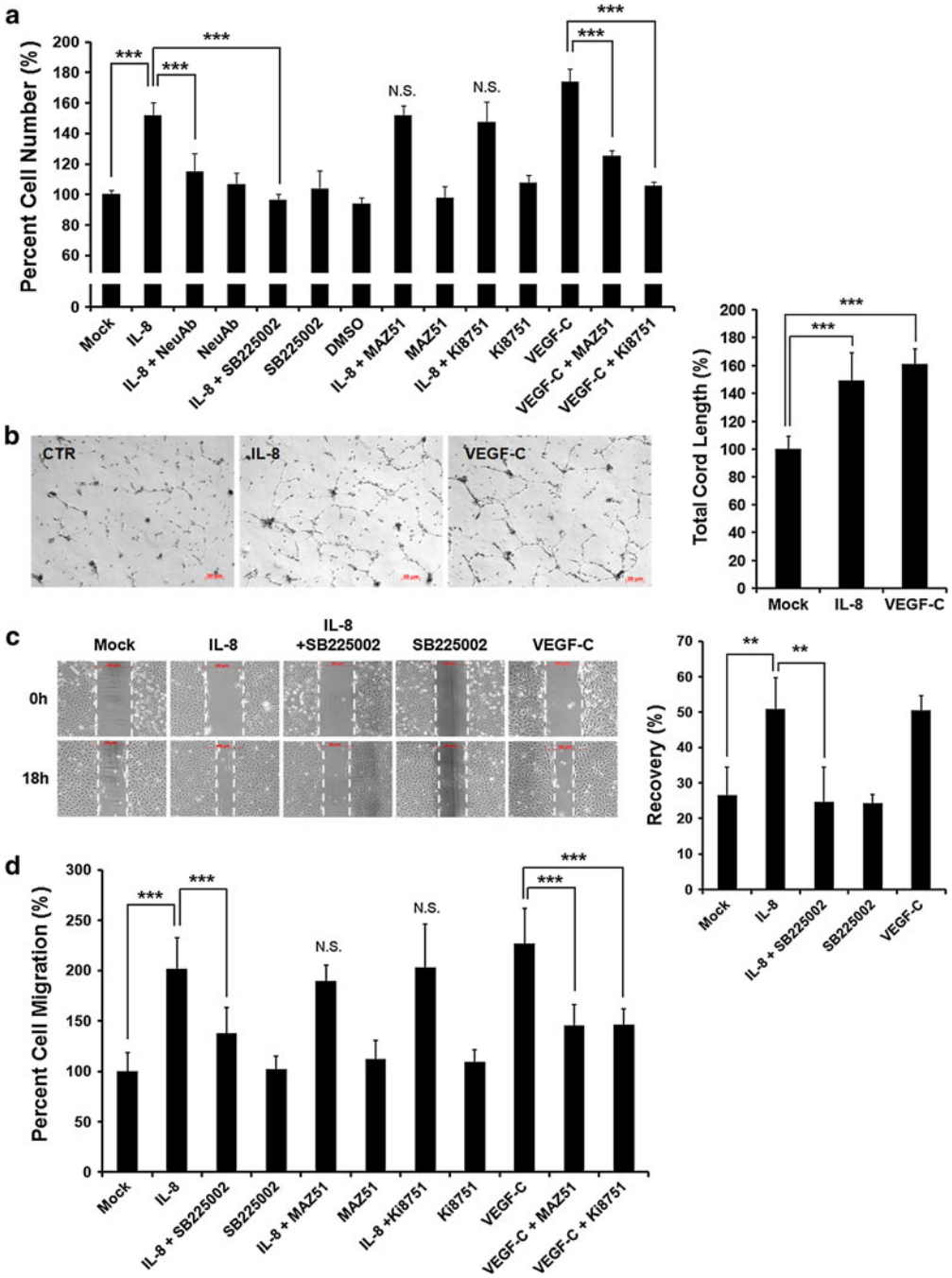

Fig. 2 IL-8 promotes proliferation, cord formation, and migration of primary LECs. **a** IL-8-activated proliferation of LECs, which was abrogated by an IL-8 neutralizing antibody (NeuAb) and SB225002, a CXCR2-specific inhibitor. A VEGFR3 kinase inhibitor, MAZ51 (50 nM), and a VEGFR2 kinase inhibitor, Ki8751 (50 nM), did not alter IL-8-activated LEC proliferation. Note that VEGF-C-induced LEC proliferation was blocked by MAZ51 and Ki8751 at the same concentration. Final cell number was calculated based on a standard curve that was prepared in parallel, and the cell number in each experimental group was normalized to a percentage against the value of the mock (PBS) -treated group (Lane 1). **b** LEC-cord formation was enhanced by IL-8. VEGF-C was used as a positive control. **c** Scratch assay showing IL-8-induced activation of LEC migration. Monolayers of LECs that were pre-treated with IL-8 or IL-8 plus SB225002 (50 nM) were wounded with pipette tips. After 24 h, total remaining wounded area was determined and expressed as a percentage of the total recovered area. PBS and VEGF-C were used as mock and positive controls, respectively. **d** Chemotactic migration assay shows increased LEC-migration by IL-8, which was diminished by SB225002, but not by MAZ51 or Ki8751. The VEGF-C-induced LEC migration was abrogated by MAZ51 and Ki8751. Modified Boyden chamber was used to assess cell migration and the resulting fluorescent values of each group was normalized to a percentage against the mock-treated group (Lane 1). All analyses were performed in quadruplicates and each experiment was repeated two times with comparable results. Data shown as an average ± standard deviation. ** $p < 0.01$; *** $p < 0.001$; *NS* not significant

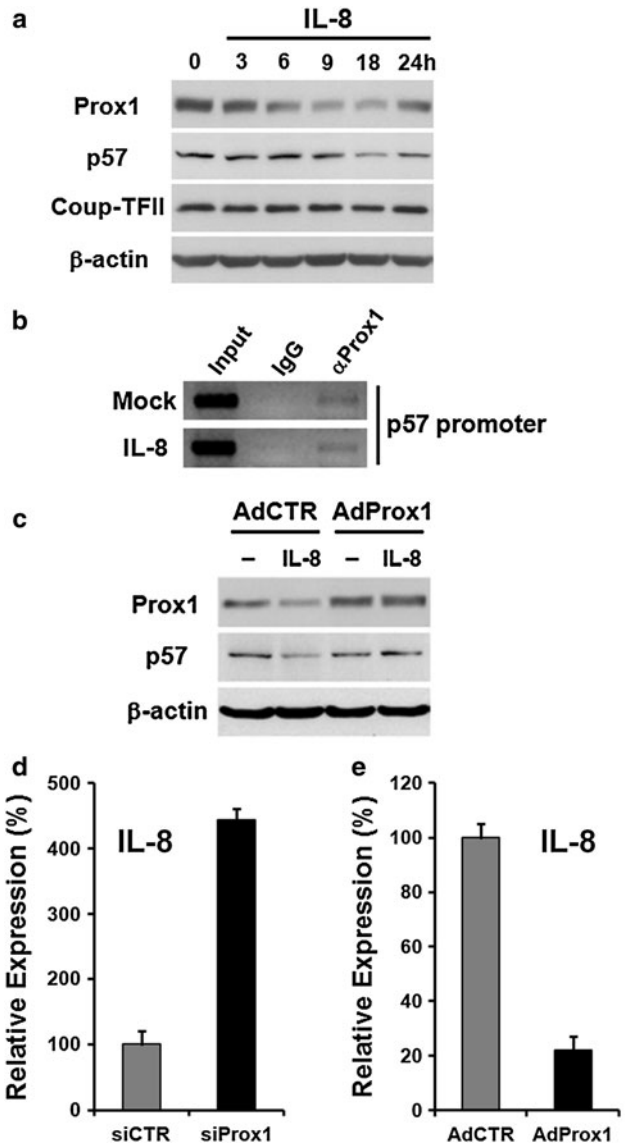

Fig. 3 IL-8 downregulates the $p57^{Kip2}$ cell cycle inhibitor by suppressing PROX1. **a** Downregulation of PROX1 and $p57^{Kip2}$ in IL-8-treated LECs. PROX1 expression was reduced after 6 h and recovered by 24-h. $p57^{Kip2}$ expression was reduced at 18 h post IL-8 treatment. Expression of COUP-TFII, a binding partner of PROX1 [32], was not affected by IL-8 treatment. **b** PROX1 ChIP assays showing a physical association of PROX1 protein with the $p57^{Kip2}$ promoter. PROX1-binding to the $p57^{Kip2}$ promoter was not affected by IL-8 treatment for 4 h. **c** Adenoviral expression of PROX1 prior to IL-8-treatment prevented the IL-8-mediated downregulation of $p57^{Kip2}$ in LECs. **d** Knockdown of PROX1 in LECs using siRNA resulted in upregulation of IL-8 expression. **e** Adenoviral overexpression of PROX1 reduced the IL-8 expression in blood vascular endothelial cells that do not express PROX1. Analyses were performed twice (*a*, *b* and *c*) or three times (*d* and *e*), with similar outcomes. The experiment was repeated with comparable data, and is shown in Supplemental Figure 2

K14-hIL8 mice by measuring its activity using a delayed-type hypersensitivity (DTH) assay [39]. DTH reactions were elicited using Oxazolone, a sensitizing agent, onto the ears of K14-hIL8 and wild-type littermates, and the progression and extent of the skin inflammation were assessed by measuring the thickness/swelling of the ears. Indeed, K14-hIL8 mice developed a relatively higher degree of skin inflammation than their wild-type littermates, as determined by vasculature and thickening of the ears (Fig. 5e,f). This finding indicates that the transgenically expressed, human IL-8 can enhance chemically-elicited skin inflammation in mice, demonstrating the functionality of human IL-8 in mouse tissues.

IL-8 enhances physiological lymphangiogenesis during embryo development

Because IL-8 is a potent pro-inflammatory cytokines that can indirectly activate lymphangiogenesis, we set out to study the direct effect of IL-8 in embryonic lymphangiogenesis, which does not involve inflammation. In order to conveniently visualize lymphatic vessels, we crossed the K14-hIL8 mouse with a lymphatic-specific GFP mouse (Prox1-GFP) [33] to generate a double transgenic mouse line (K14-hIL8/Prox1-GFP). We harvested the back skins from newborn pups (P0) of K14-hIL8/Prox1-GFP or Prox1-GFP mice, and performed quantitative vascular analyses on dermal lymphatic vessels. Indeed, K14-hIL8/Prox1-GFP mice showed a small, but statistically significant, increase in lymphatic vessel lengths and branching points, compared to Prox1-GFP mice (Fig. 6a,b). These results demonstrate that the ectopic expression of IL-8 in the skin during embryogenesis enhances developmental lymphangiogenesis.

Increased peri-tumoral lymphangiogenesis by microenvironment-derived IL-8 or CXCR2

In order to show the pro-lymphangiogenic activity of IL-8 in the post-developmental setting, we employed a tumor graft model and investigated the effect of IL-8 on tumor-associated lymphangiogenesis in adults. To avoid inflammation caused by xenografts, we established an immunodeficient K14-hIL8 mouse line (K14-hIL8/Nude) by crossing K14-hIL8 mice with athymic nude mice and then grafted either human (HCT116) or mouse (CT26) colon cancer cells in their back skins. After the cancer cells formed subcutaneous tumors (Supplemental Figure 4), we harvested them and analyzed tumor-associated lymphatic vessel formation. Importantly, the number of peri-tumoral lymphatic vessels was significantly increased in K14-hIL8/Nude mice, compared to the control nude mice, for both human and mouse cancer cells (Fig. 7a,c). In comparison, lymphatic vessel size was largely unchanged between the two groups for both cancer cell lines (Fig. 7b,d). In addition, we studied the role of the IL-8 receptor CXCR2 in tumor-associated lymphangiogenesis by syngeneically grafting CT26 cancer cells

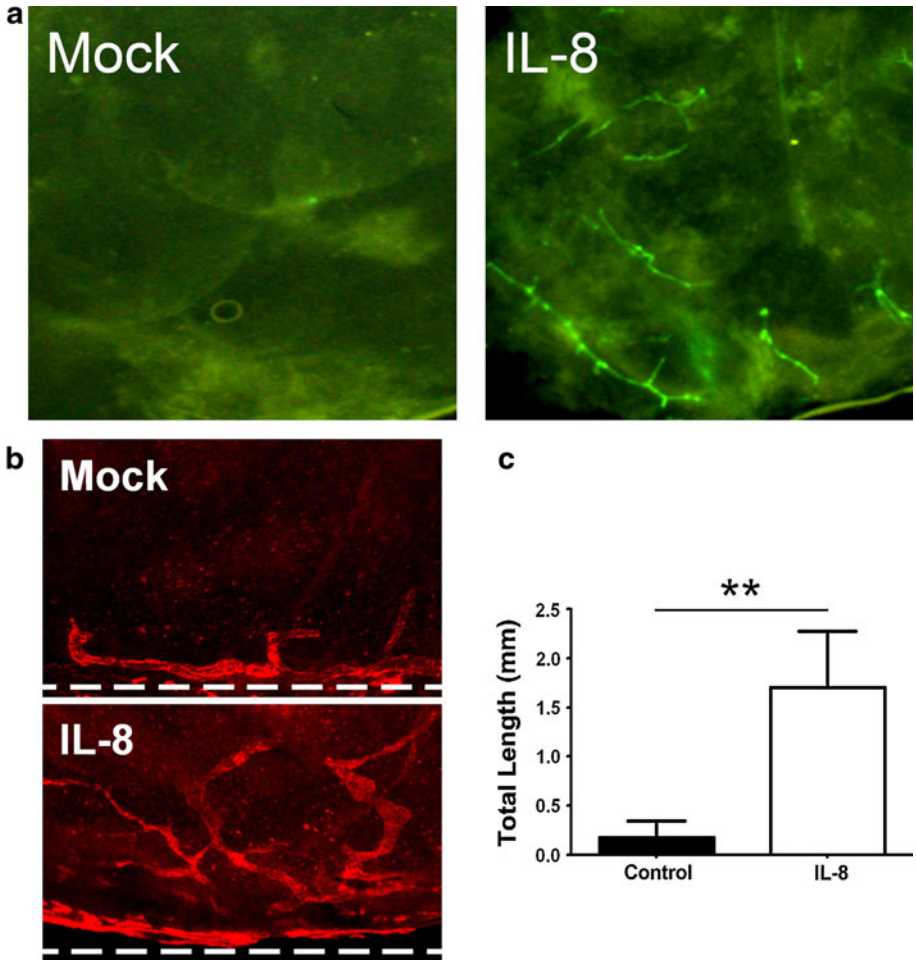

Fig. 4 Promotion of in vivo lymphangiogenesis by IL-8 **a** Matrigel plug assay showing induced in vivo lymphangiogenesis by IL-8. To directly visualize lymphatic ingrowth, lymphatic-specific GFP mice [33] were employed for matrigel plug assay. Growth factor-depleted matrigels premixed with Mock (PBS) or IL-8 (50 ng/ml) were subcutaneously inoculated into the *left* or *right flank* of the same mouse (two matrigel plugs per mouse, 5 mice per group). After 2 weeks, lymphatic vessel sprouting into the matrigels was directly visualized under a fluorescent stereoscope. Increase in the lymphatic vessel sprouting was quantified and shown in Supplemental Figure 3. This experiment was repeated twice and comparable results were obtained. **b** Mouse cornea micropocket assay was performed using wild-type mice. Lymphatic-specific LYVE-1 immunofluorescent staining demonstrates prominent ingrowth of new lymphatic vessels into the cornea in 14 days after IL-8 pellet implantation. Ten mice were used for each group (n = 10). *Dotted lines* indicate demarcation between the cornea and conjunctiva. Original Magnification: × 50. **c** The outcome of the micropocket assay was quantitatively displayed as total lymphatic length ± standard error. ** $p < 0.01$

(BALB/c-derived) in the skin of CXCR2 knockout mice on a BALB/c background. Importantly, the number of peri-tumoral, but not of intra-tumoral, lymphatic vessels was significantly decreased in CXCR2 knockout mice without any significant changes in lymphatic vessel size (Fig. 7e,f). Taken together, these studies using various mouse models demonstrate that the IL-8/CXCR2 signaling can activate post-developmental lymphangiogenesis.

IL-8 reduces experimental lymphedema by regenerating lymphatic vessels

We next evaluated the therapeutic efficacy of IL-8 using an experimental mouse tail lymphedema model that has been widely utilized as an animal model for post-surgical secondary lymphedema in humans [40]. We induced tail lymphedema by surgically obstructing the dermal lymphatic networks in the tail of male K14-hIL8 transgenic and wild-type mice, and then measured the diameters of the tails at the proximal and distal sides of the incisions over 4 weeks. Importantly, both groups showed a comparable degree of tissue swelling in their tails (averaging ~3.2 to ~5.5 mm in diameter). However, lymphedema of K14-hIL8 transgenic mice began to reduce after the first week, whereas that of wild-type mice persisted for more than 3 weeks (Fig. 8a,b). After 4 weeks, we performed IHC analyses for lymphatic vessels in the tails of the two groups and found that lymphatic regeneration was much more

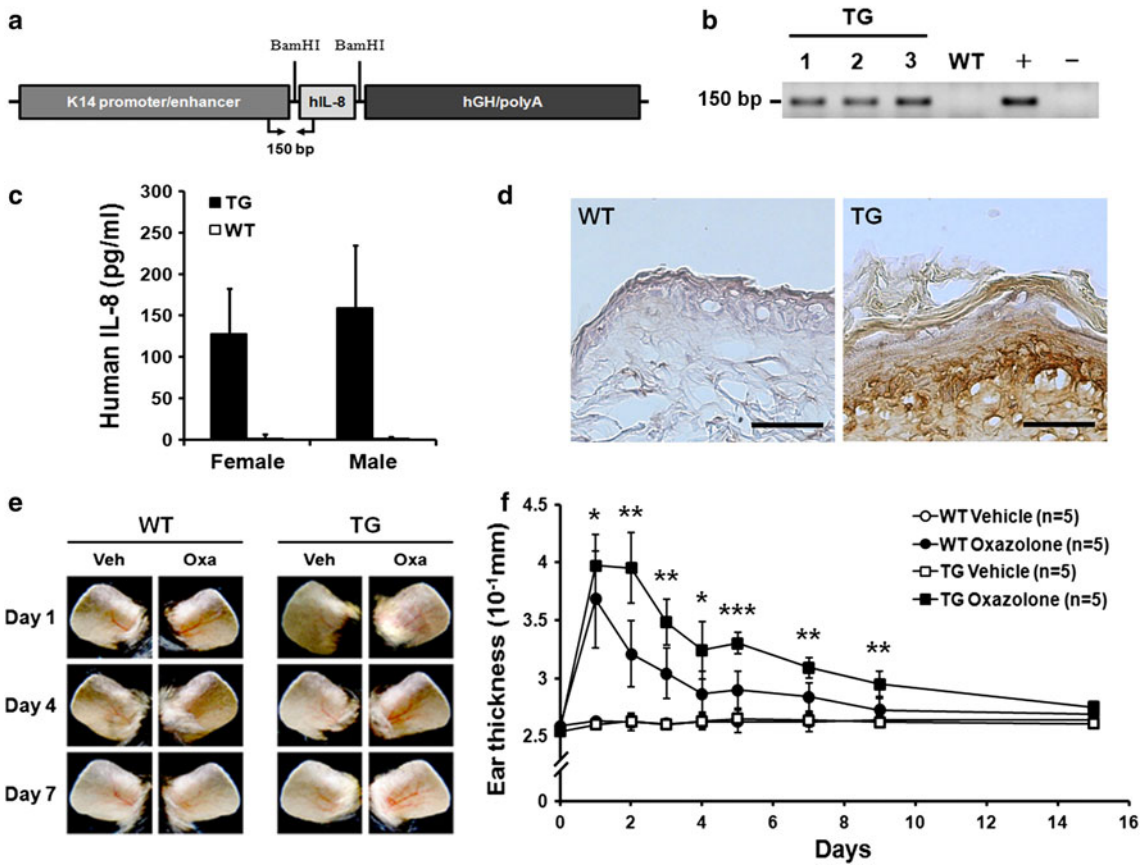

Fig. 5 Generation and characterization of a transgenic mouse expressing human IL-8 in the skin. **a** Schematic representation of the keratinocyte-specific transgene cassette expressing human IL-8 under the keratin-14 promoter. hGH, human growth hormone exons/introns. **b** PCR-based genotype analyses identified representative three founder transgenic lines (TG). Genomic DNA from wild-type mouse (WT), transgenic DNA (+) and no DNA (−) were used as controls for the genotyping assays. PCR primers located within the transgene are shown in panel **a**. **c** Secretion of IL-8 was detected in the sera of representative male or female transgenic mice using ELISA. IL-8 was not detected in wild-type mice. **d** IHC analyses demonstrating the expression of IL-8 in the transgenic mouse skin. Note a prominent secretion of IL-8 from the basal keratinocyte layer. No signal was detected in the wild-type littermates. *Scale bar*, 100 μm. **e**, **f** DTH reaction was elicited in the ears of wild-type and K14-hIL8 mice (n = 5 per group), using Oxazolone as a sensitizing agent. Left ears were treated with vehicle (Veh, ethanol) and right ears with Oxazolone (Oxa). Images (**e**) and thickness (**f**) of the ears during the DTH response are shown. DTH experiments were performed twice and similar results were obtained. * $p < 0.05$, ** $p < 0.01$, *** $p < 0.001$

prominent in K14-hIL8 transgenic mice than wild-type mice (Fig. 8c). We evaluated possible involvement of inflammation by IHC analyses for macrophages and neutrophil, as well as Hematoxylin and Eosin (H&E) staining, in the affected area, but found no signs of inflammatory involvement (Supplemental Figures 5, 6, 7). Moreover, lymphatic vascular analysis was also performed using another lymphatic marker, podoplanin (Supplemental Figure 8). Taken together, these data indicate that the IL-8 can help prevent the formation of secondary lymphedema in mouse, likely by promoting lymphatic regeneration.

Discussion

The blood and lymphatic systems are the two major circulatory systems in mammals. These two vascular systems are similar in their function and anatomy. In addition, microarray-based transcriptome studies, reported by us and others, revealed that endothelial cells from blood and lymphatic vessels show similar gene expression profiles [41–43]. Consistent with these molecular findings, many growth factors such as VEGF-A, FGF, and PDGF were found to activate both angiogenesis and lymphangiogenesis. Furthermore, various pro-inflammatory mediators can indirectly induce angiogenesis and lymphangiogenesis by activating infiltrating immune cells to secrete many lymph/angiogenic factors.

The pro-inflammatory cytokine IL-8 has been immensely studied for its functions and involvement in inflammation, tumor development and metastasis [38]. IL-8 was one of the first CXC-cytokines identified to activate angiogenesis [21, 22]. Nonetheless, the direct role of IL-8 in lymphangiogenesis has not been established to date. It has

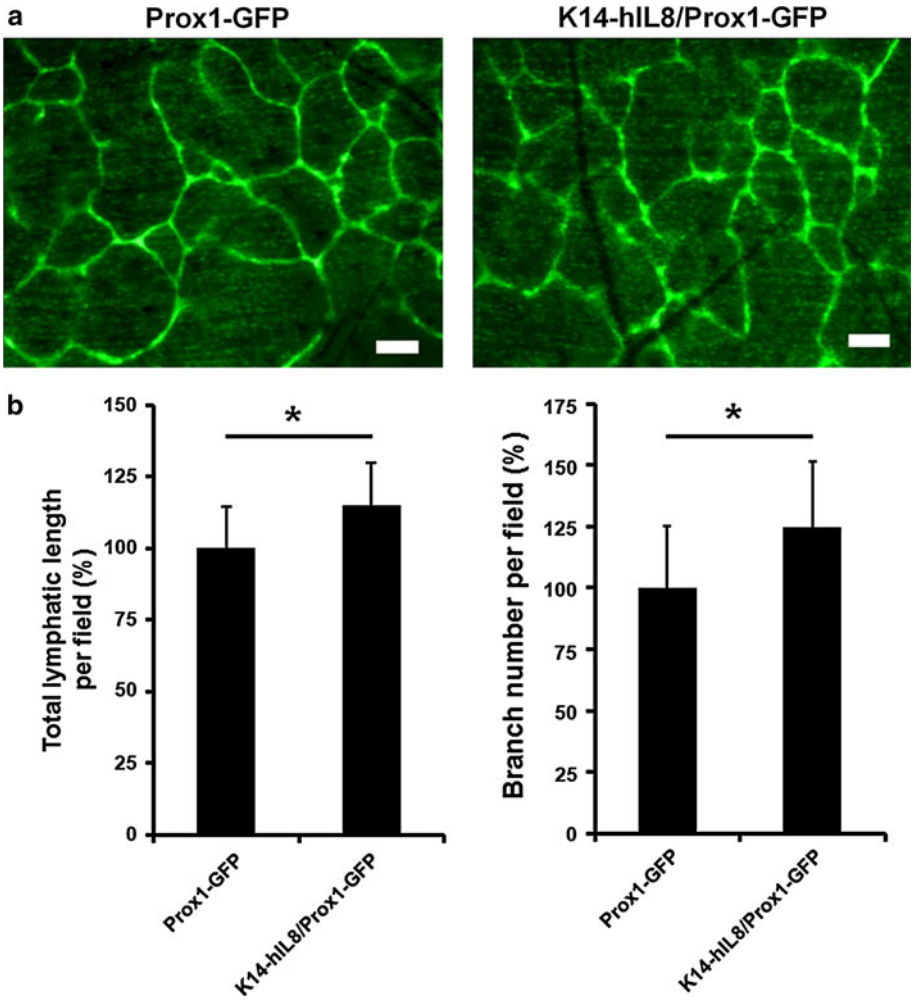

Fig. 6 Enhanced developmental lymphangiogenesis by IL-8. **a** Dermal lymphatic networks of neonatal pups of Prox1-GFP (n = 5) versus K14-hIL8/Prox1-GFP (n = 6) mice. *Scale bars*, 20 μm. **b** Morphometric vascular analyses were performed on the dermal lymphatic networks of the two groups of mice. Microscopic images of the lymphatic networks in the dorsal flank areas were captured with ten pups per group. Total length and branching points of lymphatic vessels per optical field were measured for five fields (×200) using the NIH Image J program. All values were normalized against the control (Prox1-GFP) mice and displayed as a percent average ± standard deviation. * $p < 0.05$

been difficult to investigate the direct role of IL-8 in lymphangiogenesis, as decoupling its function in lymphangiogenesis from inflammation has been challenging. In this study, we established a direct molecular link between IL-8 and lymphangiogenesis using a number of in vitro assays and novel animal models. In particular, we have generated a novel transgenic mouse line, K14-hIL8, which expresses and secretes human IL-8 specifically in the skin. Initially, multiple transgenic founders with different expression levels of IL-8 in the serum were obtained and some of them, especially those with high IL-8 level (greater than 1,000 pg/mL), occasionally developed sporadic, spontaneous skin lesions that were suspected to be caused by IL-8-induced skin inflammation. Interestingly, however, the high IL-8 expressing founders did not breed well and failed to produce any offspring. Among the remaining founders, one with ~100 pg/mL IL-8 in the serum was established as a line and was used for this study. Importantly, mice of this line did not display any signs of spontaneous skin inflammation, and are fertile without any obvious health problems. Moreover, we did not find any signs of enhanced inflammation that might affect the results of our in vivo lymphangiogenesis assays (Figs. 6, 7, 8), based on IHC against macrophages and neutrophils and high resolution H&E staining (Supplemental Figures 5, 6, 7). When we deliberately elicited inflammatory reactions, such as DTH response, human IL-8 produced from transgenic mouse skin could indeed promote the inflammatory response more prominently than wild-type littermates (Fig. 5). Notably, however, the IL8-mediated promotion of the skin inflammation in this specific K14-hIL8 line was surprisingly moderate, considering that IL-8 is one of the most potent inflammatory mediators. In comparison, a previously reported K14-VEGF mouse model, which expresses VEGF in the skin, exhibited a continuously pronounced skin inflammation for more than 4 weeks when subjected to a comparable DTH reaction [39]. We attribute this discrepancy to human IL-8 being a poor agonist for mouse IL-8 receptors [36], and also to the low serum IL-8 level in our K14-hIL8 mouse line. Consistent with this attribution, the amino acid sequence identity between human and mouse CXCR2 is only 71 % (NCBI Reference

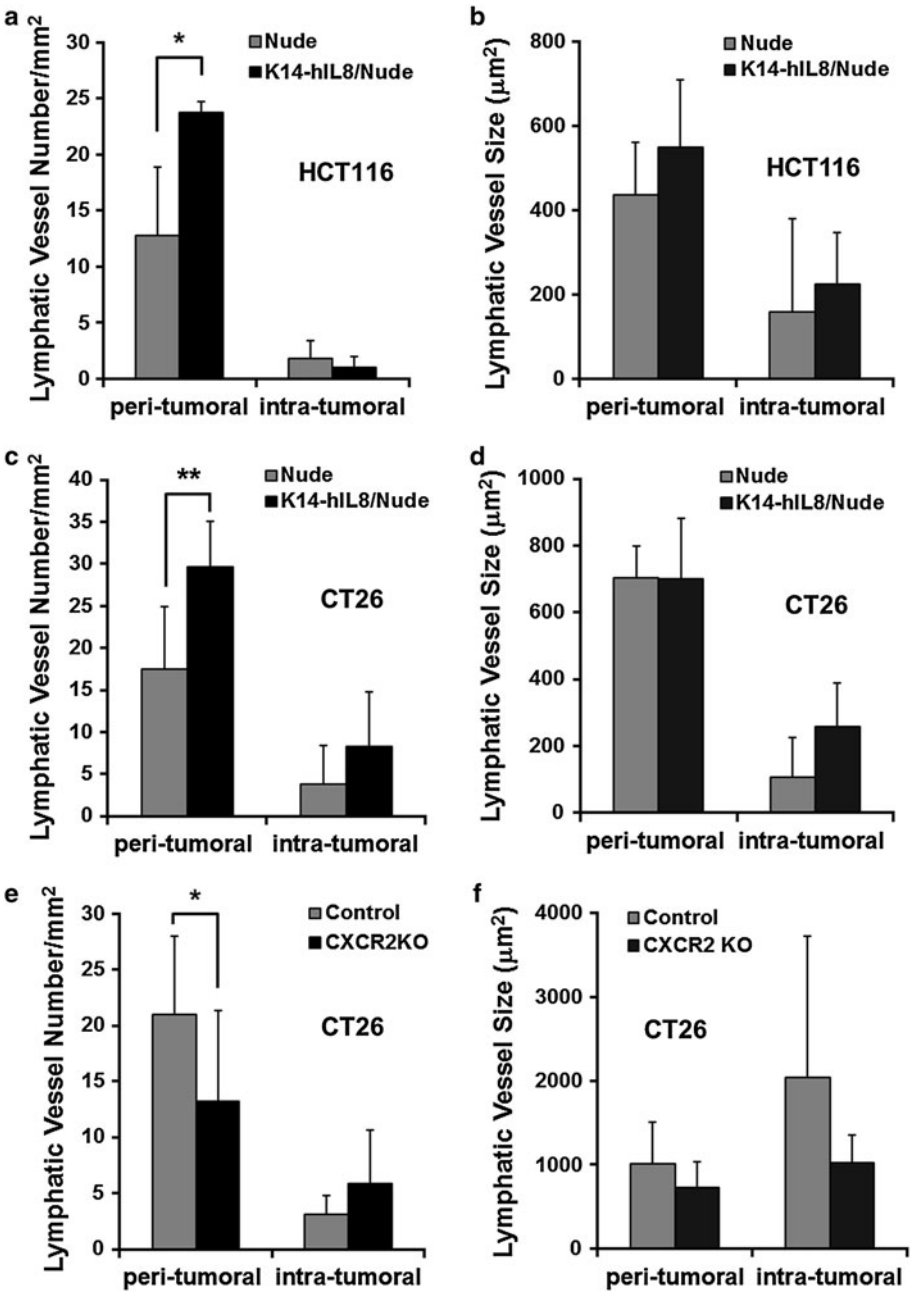

Fig. 7 Increased peri-tumoral lymphangiogenesis by IL-8/CXCR2. Vessel density (**a**,**c**) and size (**b**,**d**) of LYVE-1-positive peri-tumoral or intra-tumoral lymphatic vessels of tumors of HCT116 human colon cancer cells (**a**,**b**) or CT26 mouse colon carcinoma cells (**c**,**d**) grown in K14-hIL8/nude versus control nude mice. Six to eight mice were used per group and tumors were grown for 3 weeks. Vessel density (**e**) and size (**f**) of LYVE-1-positive lymphatic vessels in the peri-tumoral and intra-tumoral areas of CT26-induced tumors in BALB/c wild-type (n = 10) versus BALB/c CXCR2 KO (n = 10) mice. Tumor-related experiments were performed twice with comparable results. All data are displayed as an average ± standard deviation. * $p < 0.05$; ** $p < 0.01$

Sequence: NP001161770.1 vs. NP034039.1), whereas that between human and mouse VEGFR-2 proteins, the major receptor for VEGF-A, is 86 % (NP002244.1 vs. NP034742.2). It is possible that mouse Cxcr2 may have lost its affinity to IL-8 because mice do not carry an IL-8 gene in their genome [35–37]. Together, the expression level of IL-8 in our K14-hIL8 mouse line is low enough to not elicit any spontaneous inflammation, but enough to enable us to study the direct effect of IL-8 on lymphangiogenesis.

A recent study by Mu et al. [44] has elegantly demonstrated that phospholipid lysophosphatidic acid (LPA) activates the in vitro feature of lymphangiogenesis, such as LEC-proliferation, survival, migration, and tube formation. In addition, the study found that LPA upregulates IL-8 by enhancing the IL-8 promoter activity via activation of the NF-kB pathway in LECs, and that IL-8 plays an essential role in the LPA-induced lymphangiogenesis. The authors also detected the expression of IL-8 receptors in LECs and proposed a direct effect of IL-8 in lymphangiogenesis. We hypothesize that the regulation of IL-8 by LPA and the function of IL-8 in LPA-induced lymphangiogenesis are highly consistent with the upregulation of IL-8 by 9-cisRA (Fig. 1c,d) that has been shown to activate lymphangiogenesis in vitro and in vivo [27]. Together, these findings highlight the role of IL-8-mediated autocrine activation of

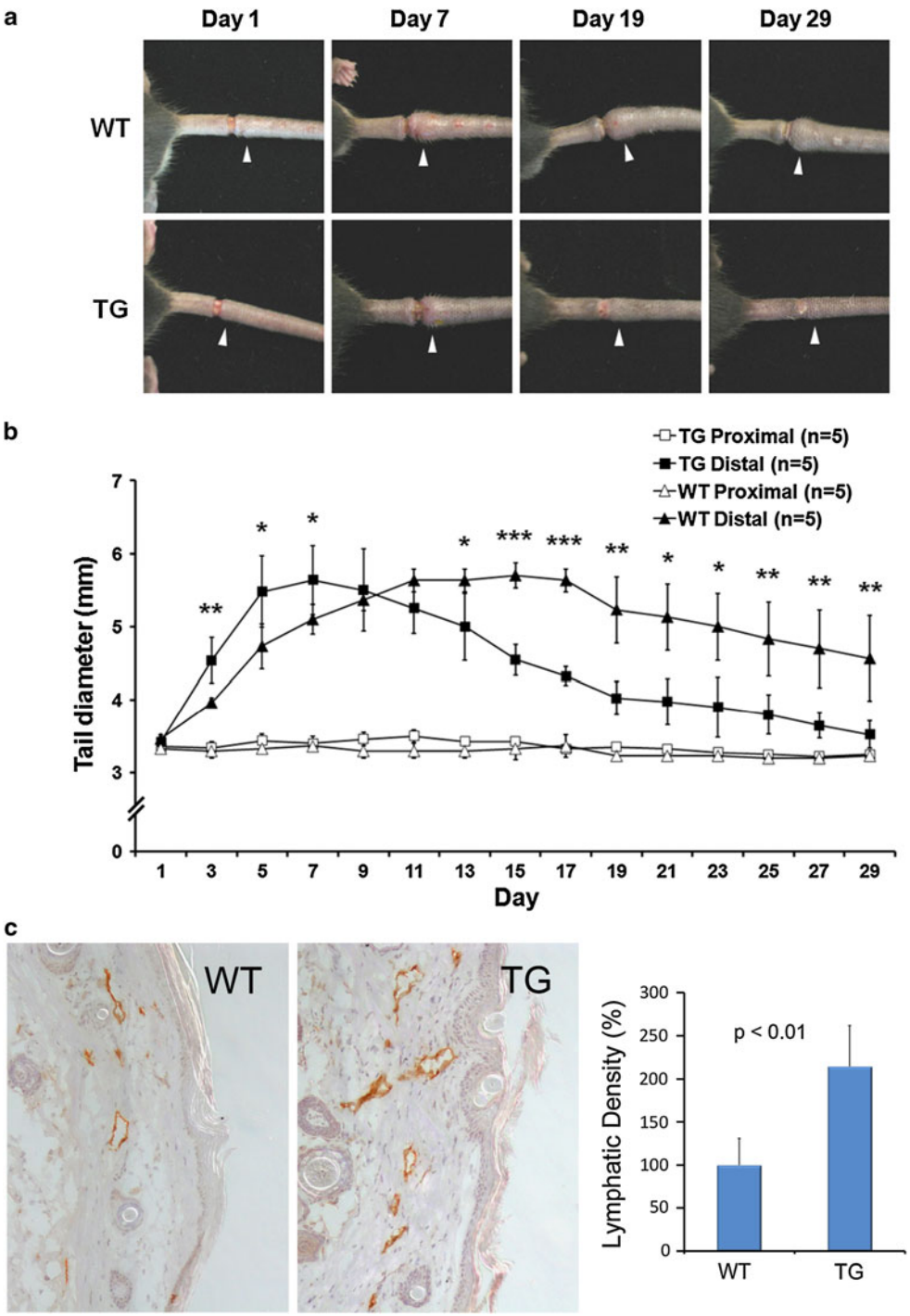

Fig. 8 IL-8 effectively ameliorates secondary lymphedema by regenerating lymphatic vessels. **a** Representative images showing development of secondary lymphedema in the tail of wild-type mice (WT) (n = 5) versus K14-hIL8 transgenic (TG) (n = 5) mice for 29 days. *White arrowheads mark* the edematous regions of the tails. **b** Diameter of the distal (edematous) and proximal (reference) sides of the wounds were measured every other day. Five mice were used for each group. Data displayed as an average ± standard deviation. * $p < 0.05$; ** $p < 0.01$; *** $p < 0.001$. **c** The tails were harvested after 29 days and subjected to IHC analyses. An increased regeneration of LYVE-1-positive lymphatic vessels was observed in K14-hIL8 mice (TG) compared to wild-type group (WT). Lymphatic vessel density was measured for a total of five fields per group. This experiment was repeated two times with similar outcomes

LECs in lymphangiogenesis, that is induced by various stimuli such as LPA and retinoic acids.

IL-8 has been shown to stimulate the expression of VEGF and the autocrine activation of VEGFR signaling in vascular endothelial cells [24]. Importantly, we found that IL-8-induced activation of proliferation and migration of LECs did not involve the VEGFR signaling (Fig. 2). This finding suggests that the molecular mechanisms underlying IL-8-mediated activation of angiogenesis versus lymphangiogenesis may not be identical, despite a close histogenetic relationship between these two endothelial cell types. Supporting this notion, another important finding in this study is the regulation of $p57^{Kip2}$ and its positive regulator PROX1 by IL-8 (Fig. 3). Several studies have previously established that PROX1 acts a positive regulator of $p57^{Kip2}$ by directly binding to the promoter of the gene [27, 41, 45–48]. IL-8 treatment resulted in downregulation of $p57^{Kip2}$ in LECs and this downregulation of $p57^{Kip2}$ required the suppression of its positive regulator

PROX1 because ectopic expression of PROX1 prevented the IL-8-mediated downregulation of $p57^{Kip2}$ (Fig. 3c, Supplemental Figure 2). Recently, we reported that 9-cis retinoic acid downregulates $p57^{Kip2}$ expression by dissociating PROX1 protein from the $p57^{Kip2}$ promoter within 1 h of treatment [27]. To our surprise, the occupancy of PROX1 protein in the $p57^{Kip2}$ promoter was not altered by IL-8 (Fig. 3b), suggesting that IL-8 suppresses $p57^{Kip2}$ expression by regulating the expression, not DNA binding affinity, of PROX1. Furthermore, the expression of $p27^{Kip1}$, another cell cycle inhibitor shown to be regulated by 9-cis retinoic acid [27], was not affected by IL-8 (data not shown). Together, we conclude that downregulation of $p57^{Kip2}$ by IL-8 via PROX1 may play a key role in the IL-8-promoted LEC proliferation.

On the other hand, the finding that PROX1 represses the expression of IL-8 establishes a reciprocal regulation between PROX1 and IL-8 (Fig. 3). It is noteworthy to find that LECs express and secrete a considerably high level of IL-8 ($\sim$500 pg/mL media) under normal culture conditions (Fig. 1). Considering both the chemotactic role of IL-8 and the immune cell-draining function of lymphatic vessels, LECs may need to secrete a high level of IL-8 to chemo-attract and drain leukocytes to lymph nodes for immune reactions. One could imagine a scenario where a small amount of IL-8, which may be supplied by transient immune cells, could trigger a de novo amplification cycle of IL-8 expression in LECs by removing the inhibitory effect of PROX1 on IL-8 expression, which then leads to an increased production of IL-8 from LECs. Moreover, this IL-8 amplification cycle appears to be associated with both downregulation of the cell cycle inhibitor, $p57^{Kip2}$, and LEC proliferation. The de novo amplification cycle of IL-8 expression in LECs does not seem to last long as PROX1 expression reduced at 18-h was soon recovered by 24 h (Fig. 3).

Experiments using our animal models confirmed the in vitro lymphangiogenic activity of IL-8, independent of its pro-inflammatory activity. Mouse matrigel plug and cornea micropocket assays clearly demonstrated that IL-8 strongly induced lymphatic vessel growth in vivo (Fig. 4). The transgenic animal models demonstrated the pro-lymphangiogenic activity of IL-8 for embryonic lymphatic development, as well as post-developmental tumor-associated lymphangiogenesis (Figs. 5, 6, 7). Importantly, our K14-hIL8 model allowed a steady and constant systemic supply of human IL-8 and enabled us to investigate the therapeutic efficacy of IL-8 using mouse tail lymphedema, a widely employed animal model of human lymphedema [40]. Consistent with its activity in vitro and in vivo lymphangiogenesis, IL-8 was effective in resolving tissue swelling by inducing lymphatic vessel regeneration. Although lymphedema was comparably developed in the tails of both control and K14-hIL8 mice, the steady supply of IL-8 accelerated the resolution of the secondary lymphedema with increased lymphatic vessel regeneration, whereas the control wild-type group exhibited prominent lymphedema even at week 4. It is worth mentioning that inflammation was not involved in this process as there were no signs of inflammation detected during the course of lymphedema resolution (Supplemental Figures 5, 6, 7). Another support for the lack of inflammation comes from our lymphedema study (Fig. 8), as it is known that inflammation stimulates vascular leakage and induces tissue fluid accumulation (swelling). However, our K14-hIL8 mice displayed better resolution of tissue swelling compared to wild-type mice. If inflammation were involved, it should increase the volume of tissue swelling, exacerbating the edematous state, rather than ameliorating the condition.

In summary, our current study newly defines the pro-lymphangiogenic activity of IL-8 and establishes its therapeutic efficacy in secondary lymphedema. Moreover, our molecular analyses revealed a lymphatic-specific functional mechanism underlying the IL-8-mediated LEC proliferation that may not operate in blood vascular endothelial cells. Considering the fact that there is no effective treatment available to date for this disfiguring and painful illness, IL-8, one of the best studied cytokines, deserves further studies exploring its therapeutic usage in treating human lymphedema patients.

Materials and methods

Cell culture, reagents and gene expression

Human primary LECs were isolated from neonatal foreskins with pre-approval by the Institutional Review Board, University of Southern California (PI: Hong), and cultured in a complete media as previously described [49]. LECs less than 8-population doublings (passages) were used for all experiments in this study. The BALB/c-derived mouse colon adenocarcinoma CT26 and human HCT116 were purchased from American Type Culture Collection (ATCC). Human recombinant TNF-α and IL-8 were purchased from R&D systems (Minneapolis, MN). 9-cis retinoic acid was purchased from Sigma-Aldrich (St. Louis, MO). Conventional reverse transcription polymerase chain reaction (RT-PCR) was performed using Superscript II (Invitrogen, Carlsbad, CA) and *Taq* polymerase (Finnzymes, Finland). Primer sequences will be provided upon request. Sources of antibodies for western blot analyses are: anti-p27 (Santa Cruz Biotechnology, sc-528), anti-p57 (Santa Cruz Biotechnology, KP39), anti-PROX1 (rabbit polyclonal antibody generated by the authors), anti-COUP-TFII (Perseus Proteomics, H7147, Japan) and anti-β-actin (Sigma-Aldrich, AC-15). Control and PROX1 adenovirus were previously described [16].

IL-8 ELISA

To measure the level of secreted IL-8, primary LECs were seeded onto 6-well plates and cultured overnight in EBM containing 1 % FBS. Equal volume of PBS, ethanol or 9-cisRA (1 μM) was added for 24 h, and the media was then harvested to determine the concentration of secreted proteins using an ELISA kit (R&D Systems).

Immunofluorescence & IHC analyses

Cells were attached to collagen-coated cover slips, washed in phosphate buffered saline (PBS), fixed with 4 % paraformaldehade (PFA) for 20 min, incubated in a blocking buffer (0.5 % bovine serum albumin in PBS) for 1 h at room temperature, and followed by overnight incubation with anti-PROX1 (ReliaTech, Germany), anti-CXCR1 (Cell Applications, CA0755), and anti-CXCR2 (Cell Applications, CA0757) antibodies. Cells were then rinsed with PBS, incubated with fluorescence-conjugated secondary antibodies (Invitrogen), rinsed three times with PBS and mounted on glass slides using Vectashield medium (Vector Laboratories, Burlingame, CA) containing DAPI (4,6-diamidino-2-phenylindole). Images were taken using a fluorescence microscope (Zeiss, Germany). Sources of antibodies used for IF/IHC studies were anti-CD31 (BD Bioscience, San Jose, CA; MEC13.3), anti-LYVE-1 (Abcam, Cambridge, MA; ab14917), anti-macrophage (eBioscience, F4/80), anti-neutrophil/Gr1 (Santa Cruz Biotechnology, sc-53515), and anti-podoplanin (Hybridoma bank, 8.1.1).

Proliferation assay

Endothelial cell proliferation assay was performed using a Premixed WST-1 Cell Proliferation Assay kit (TaKaRa, Japan), following the manufacturer's instruction. In brief, human primary LECs were seeded at a concentration of 2×10^4 cells per well in 24-well plates and cultured overnight. The media was then replaced with fresh media (1 % serum) containing IL-8 (10 ng/ml) or no IL-8 as a control. Cells were then allowed to grow for 48 h, where the cell proliferation reagent WST-1 was then added to each well and incubated for an additional 4 h. Optical absorbance was subsequently measured at a wavelength of 450 nm using a microplate reader (Hidex Chameleon V, Finland), and the cell proliferation count was estimated based on a standard curve that was prepared in parallel. The receptor inhibition study was performed by incubating LECs with IL-8 in the presence of anti-IL-8 neutralizing antibody (R&D Systems, AF-208-NA), SB225002 (CXCR2 inhibitor, Calbiochem, Germany), MAZ51 (VEGFR3 kinas inhibitor, Sigma-Aldrich), or Ki8751 (VEGFR2 kinase inhibitor, Sigma-Aldrich). VEGF-C (R&D systems) was used as a positive control.

Migration assay

Cell migration assay was performed using HTS Fluoroblok™ Multiwell Insert System (BD Falcon, Franklin Lakes, NJ). The bottom of the Fluoroblok inserts were coated with a collagen (50 μg/mL) solution containing 0.01 % delipidized BSA (Sigma-Aldrich) for 30 min. 5×10^4 cells of human primary LECs were resuspended in 200 μL basal media containing 0.2 % delipidized BSA and added to the upper chamber. 500 μL of basal media containing 0.2 % delipidized BSA was added in the lower chamber along with either PBS or IL-8 (10 ng/ml). After 3-h of incubation at 37 °C, the migrated cells at the bottom side of the insert were stained with 2 μM Calcein AM (Invitrogen) at 37 °C for 10 min. The Fluoroblok™ inserts were then washed in PBS and fixed with 4 % PFA. Fluorescence intensity was measured using a fluorometer (Hidex Chameleon V) and images were captured using a Zeiss fluorescent microscopy.

Endothelial tube formation and scratch assays

Human LECs were pre-treated with or without IL-8 (10 ng/ml) for 24 h. Separately, 200 μL of growth factor-depleted Matrigel™ (BD Bioscience) were placed into a pre-chilled 12-well plate and solidified for 30 min at 37 °C. Pre-treated LECs (5×10^4) cells were overlaid on the Matrigel™ in fresh media. Cord formation was observed after 6 h, representative images were randomly taken at 24 h, and total length of formed cord therein was measured using the NIH Image J program. For the scratch assay, primary human LECs (4×10^5) were seeded in 60-mm dishes and pre-treated with PBS, IL-8 (10 ng/ml), or IL-8 plus SB225002 for 24 h. VEGF-C was used as a positive control. A confluent monolayer was scratched using a 1,000-μL pipette tip and incubated for an additional 24 h. The migrated cell images were captured and analyzed to determine the average remaining wound area using the NIH Image J program.

Chromatin immunoprecipitation (ChIP)

Assays were performed following a published protocol [50]. Briefly, genomic DNA of LECs were fragmented by sonication using a Misonix model XL2000 sonicator and the pre-cleared extracts were immunoprecipitated with a rabbit anti-PROX1 (generated by the authors) or rabbit IgG (Sigma Aldrich) antibody at 4 °C overnight. Genomic DNA was isolated from precipitated complexes, de-cross-linked, and analyzed using PCR primers for human $p57^{KIP2}$

promoter (ATCATGGCTTTTGGTTCCAC/CAGGGAAG CGAGATCTGAAG).

Corneal micropocket and matrigel plug assays

Six to eight-week-old male BALB/c mice (Jackson Laboratory, Bar Harbor, ME) were used for the experiments. For corneal micropocket assays, all mice were treated according to ARVO Statement for the Use of Animals in Ophthalmic and Vision Research, and all protocols were pre-approved by the Animal Care and Use Committee, University of California, Berkeley. Mice were anesthetized using a mixture of ketamine, xylazine, and acepromazine (50 mg, 10 mg, and 1 mg/kg body weight, respectively) for each surgical procedure. The mouse corneal micropocket assay was performed as described previously [27, 51–55]. Briefly, an initial half thickness linear incision was made at the center of the cornea using a disposable ophthalmic microknife. Using a modified Von Graefe knife, a lamellar pocket incision was then made parallel to the corneal plane and advanced to the temporal limbus at the lateral canthal area. The pellets were positioned into the pocket 1.0 mm apart from the limbal vascular arcade. A slow-release pellet of uniform size (0.3 mm) was implanted into each pocket. The pellet was made of sucralfate (Sigma-Aldrich) and hydro polymer (Sigma-Aldrich) containing either recombinant IL-8 (10 ng) or vehicle (water) alone. Ten mice were used for each group ($n = 10$). Antibiotic ointment (tetracycline) was applied to the eye after pellet implantation and the pellet was left in place for 14 days. Freshly excised corneas were fixed in acetone for immunofluorescent staining. Non-specific staining was blocked with anti-Fc CD16/CD32 antibody (BD Biosciences). The samples were stained overnight with purified rabbit anti-mouse LYVE-1 antibody (Abcam), which was visualized by a rhodamine-conjugated donkey anti-rabbit secondary antibody. Samples were covered with Vector Shield mounting medium (Vector Laboratories) and examined by an epifluorescence deconvolution microscope. Vascular structures positively stained for LYVE-1 were defined as lymphatic vessels. Lymphatic vessels were graded and analyzed using the NIH Image J software as described previously [56]. The total length was obtained by summing the length of each lymphatic vessel penetrating the cornea in the pellet area. Statistical significance was evaluated using the Mann–Whitney test with GraphPad Prism® software (GraphPad Software, Inc., La Jolla, CA).

For matrigel plug assay (Fig. 4a), 250 μL of growth factor-depleted matrigel (BD Bioscience) premixed with PBS or IL-8 (50 ng/ml) was subcutaneously injected into the lymphatic-specific fluorescent transgenic (Prox1-GFP) mice [33]. After 2 weeks, the implants were recovered and extensively cleaned by removing surrounding fat and tissues debris. Subsequently, the matrigel implants were pressed down with cover glasses to flatten them as much as possible for better visualization of the newly formed lymphatic networks.

Generation of a skin-specific IL8-expressing transgenic mouse (K14-hIL8)

A 0.3-kb human IL-8-coding fragment was PCR-amplified from a pUC19/human IL-8 vector (AddGene, Cambridge, MA) using primer sets containing BamHI site, and subsequently cloned into a unique BamHI site of the keratin 14 expression vector [57] (kindly provided by Dr. Elaine Fuchs, The Rockefeller University). The keratin 14-promoter-driven human IL-8 expression cassette was digested using KpnI and HindIII and subsequently used for pronuclear injection by the USC Transgenic Animal Core. The founders were screened for their genotypes and serum IL-8 level; one founder was chosen to establish the K14-hIL8 line.

Delayed-type hypersensitivity (DTH)

Assay was performed as previously described [39]. Contact hypersensitivity was induced in the ear skin of 8-week-old wild-type mice or K14-hIL8 transgenic mice ($n = 5$ per group). Mice were sensitized by topical application of a 2 % Oxazolone (4-ethoxymethylene-2 phenyl-2-oxazoline-5-one; Sigma-Aldrich) solution (in acetone/seed oil (4:1 vol/vol)) onto the shaved abdomen (50 μL) and to each paw (5 μL). Five days after sensitization (day 0), the right ears were treated with 20 μL of a 1 % Oxazolone solution, whereas the left ears were treated with the vehicle alone. The ear thickness was measured for up to 15 days. The unpaired Student *t* test was used for statistical analysis.

Generation of K14-hIL8/Nude mice and tumor growth experiments

For tumor growth study, we generated an immunodeficient skin-specific IL-8-expressing mouse line (K14-hIL8/Nude) by crossing K14-hIL8 mice with athymic nude mice (Crl:NU-Foxn1nu, Charles River Laboratories International, Inc. (Wilmington, MA)). Nude mice with hemizygote K14-hIL8 transgene were screened using PCR-amplification (GGCCCAGCAGGCAGCCCAAG/AGGGATCTCCTCAAAGGCTTC) for the Foxn1nu allele. Digestion of the PCR products with BseDI provided genotype-specific diagnostic patterns of DNA fragments in 5 % agarose gels for wild-type (90, 53 and 20 bp), heterozygote (20, 53, 58, 90 and ~110 bp) and mutant (~110 and 58 bp). Five outbred mice in at least the fourth generation were used per each group for the study. CXCR2

knockout (KO) mice on the BALB/c background (C.129S2(B6)-Cxcr2tm1Mwm/J) were purchased from the Jackson Laboratory (Bar Harbor, MN). 2×10^5 cells of CT26 (mouse colon cancer cells) or 1×10^6 cells of HCT116 (human colon cancer cells) were injected into the right and left flanks of control nude mice or K14-hIL8/Nude mice (five mice per group). Tumor volume was measured by width and length by a digital caliper (0.1 mm increments) every 2 days until mice were sacrificed. Mouse weight was also taken to check experimental condition.

Vascular analyses

For the vascular analyses of neonatal pups (Fig. 6), the back skins (flank area) of Prox1-GFP and K14-hIL8/Prox1-GFP neonatal pups ($n > 5$ per group) were harvested and lymphatic vessels were directly visualized using a fluorescent stereoscope. Five microscopic fields were randomly selected and their images were used for vascular analyses. Using NIH ImageJ, total lymphatic vessel length per field and total branch number per field were calculated and converted to a percentage based on the values from Prox1-GFP mice. For the tumor-related vascular analyses (Fig. 7), harvested tumor samples were processed for IHC analyses by embedding into paraffin. Anti-LYVE-1 (Angiobio, Del Mar, CA) and anti-human IL-8 (BioLegend, San Diego, CA) antibodies were used. IHC images were captured using AxioImager Z1 microscope (Zeiss, Germany). For the tumoral vascular analyses, we took images of 5–8 hot spots in the peri-tumoral area, counted total lymphatic vessel number and size using the NIH Image J software.

Mouse tail lymphedema model

The protocols for the mouse lymphedema model were pre-approved by the Institutional Animal Care and Use Committee (IACUC) of the University of Southern California. We essentially followed the previously established method for inducing lymphedema in the tails of mice [40] using wild-type C57BL/6 J mice ($n = 5$) purchased from the Jackson Laboratory (Bar Harbor, ME) and K14-IL-8 transgenic mice ($n = 5$). Briefly, under a dissectioin microscope, we removed a circumferential 2-mm-wide piece of skin located approximately 1 cm distal of the tail base. The diameter of the proximal and distal sides of the surgical site in the tail was measured every other day. At the end of the experiments, mice tails were surgically removed and processed for IHC analyses with anti-LYVE-1 (Angiobio, Del Mar, CA). IHC images were analyzed using the NIH ImageJ software. This experiment was repeated twice with similar results.

Statistical analysis

The resulting measurements were expressed as mean ± standard deviation (SD) for each experiment, except Fig. 4b, where mean ± standard error was used. All analyses were performed in quadruplicates and each experiment was repeated at least two times. Student *t* test was used to determine statistical significance between the experimental and control groups for both in vitro and in vivo studies. All reported P values were two-sided with a statistical significance level of less than 0.05. Analyses were performed using Microsoft Excel (Microsoft Office) or SAS statistical package version 9.2 (SAS Institute Inc., Cary, North Carolina).

Acknowledgments This study was supported by NIH/NICHD (YKH), American Cancer Society (YKH), American Heart Association (YKH), March of Dimes Foundation (YKH), Daniel Butler Memorial Fund (HJL), Teri Lanni Research Fund (HJL), and NIH/NEI (LC).

Conflict of interest None.

References

1. Oliver G, Alitalo K (2005) The lymphatic vasculature: recent progress and paradigms. Annu Rev Cell Dev Biol 21:457–483
2. Norrmen C et al (2011) Biological basis of therapeutic lymphangiogenesis. Circulation 123(12):1335–1351
3. Schmitz KH et al (2012) Prevalence of breast cancer treatment sequelae over 6 years of follow-up: the pulling through study. Cancer 118(8 Suppl):2217–2225
4. Shimoda H, Bernas MJ, Witte MH (2011) Dysmorphogenesis of lymph nodes in Foxc2 haploinsufficient mice. Histochem Cell Biol 135(6):603–613
5. Shah C, Vicini FA (2011) Breast cancer-related arm lymphedema: incidence rates, diagnostic techniques, optimal management and risk reduction strategies. Int J Radiat Oncol Biol Phys 81(4):907–914
6. Warren AG et al (2007) Lymphedema: a comprehensive review. Ann Plast Surg 59(4):464–472
7. Petrek JA et al (2001) Lymphedema in a cohort of breast carcinoma survivors 20 years after diagnosis. Cancer 92(6):1368–1377
8. Hardin R, Jacobs LK (2012) Lymphedema: still a problem without an answer. Oncology (Williston Park) 26(3):256–257
9. McLaughlin SA (2012) Lymphedema: separating fact from fiction. Oncology (Williston Park) 26(3):242–249
10. Tammela T, Alitalo K (2010) Lymphangiogenesis: molecular mechanisms and future promise. Cell 140(4):460–476
11. Oh SJ et al (1997) VEGF and VEGF-C: specific induction of angiogenesis and lymphangiogenesis in the differentiated avian chorioallantoic membrane. Dev Biol 188(1):96–109
12. Hong YK et al (2004) VEGF-A promotes tissue repair-associated lymphatic vessel formation via VEGFR-2 and the alpha1beta1 and alpha2beta1 integrins. FASEB J 18(10):1111–1113
13. Nagy JA et al (2002) Vascular permeability factor/vascular endothelial growth factor induces lymphangiogenesis as well as angiogenesis. J Exp Med 196(11):1497–1506
14. Nagy JA et al (2002) VEGF-A induces angiogenesis, arteriogenesis, lymphangiogenesis, and vascular malformations. Cold Spring Harb Symp Quant Biol 67:227–237

15. Nakao S et al (2010) Lymphangiogenesis and angiogenesis: concurrence and/or dependence? Studies in inbred mouse strains. FASEB J 24(2):504–513
16. Shin JW et al (2006) Prox1 promotes lineage-specific expression of fibroblast growth factor (FGF) receptor-3 in lymphatic endothelium: a role for FGF signaling in lymphangiogenesis. Mol Biol Cell 17(2):576–584
17. Cao R et al (2004) PDGF-BB induces intratumoral lymphangiogenesis and promotes lymphatic metastasis. Cancer Cell 6(4):333–345
18. Kajiya K et al (2005) Hepatocyte growth factor promotes lymphatic vessel formation and function. EMBO J 24(16):2885–2895
19. Banziger-Tobler NE et al (2008) Growth hormone promotes lymphangiogenesis. Am J Pathol 173(2):586–597
20. Bjorndahl M et al (2005) Insulin-like growth factors 1 and 2 induce lymphangiogenesis in vivo. Proc Natl Acad Sci USA 102(43):15593–15598
21. Koch AE et al (1992) Interleukin-8 as a macrophage-derived mediator of angiogenesis. Science 258(5089):1798–1801
22. Strieter RM et al (1992) Interleukin-8. A corneal factor that induces neovascularization. Am J Pathol 141(6):1279–1284
23. Simonini A et al (2000) IL-8 is an angiogenic factor in human coronary atherectomy tissue. Circulation 101(13):1519–1526
24. Martin D, Galisteo R, Gutkind JS (2009) CXCL8/IL8 stimulates vascular endothelial growth factor (VEGF) expression and the autocrine activation of VEGFR2 in endothelial cells by activating NFkappaB through the CBM (Carma3/Bcl10/Malt1) complex. J Biol Chem 284(10):6038–6042
25. Murdoch C, Monk PN, Finn A (1999) Cxc chemokine receptor expression on human endothelial cells. Cytokine 11(9):704–712
26. Li A et al (2003) IL-8 directly enhanced endothelial cell survival, proliferation, and matrix metalloproteinases production and regulated angiogenesis. J Immunol 170(6):3369–3376
27. Choi I et al (2012) 9-cis retinoic acid promotes lymphangiogenesis and enhances lymphatic vessel regeneration: therapeutic implications of 9-cis retinoic Acid for secondary lymphedema. Circulation 125(7):872–882
28. White JR et al (1998) Identification of a potent, selective non-peptide CXCR2 antagonist that inhibits interleukin-8-induced neutrophil migration. J Biol Chem 273(17):10095–10098
29. Kubo K et al (2005) Novel potent orally active selective VEGFR-2 tyrosine kinase inhibitors: synthesis, structure-activity relationships, and antitumor activities of N-phenyl-N'-{4-(4-quinolyloxy)phenyl}ureas. J Med Chem 48(5):1359–1366
30. Kirkin V et al (2004) MAZ51, an indolinone that inhibits endothelial cell and tumor cell growth in vitro, suppresses tumor growth in vivo. Int J Cancer 112(6):986–993
31. Baxter SA et al (2011) Regulation of the lymphatic endothelial cell cycle by the PROX1 homeodomain protein. Biochim Biophys Acta 1813(1):201–212
32. Lee S et al (2009) Prox1 physically and functionally interacts with COUP-TFII to specify lymphatic endothelial cell fate. Blood 113(8):1856–1859
33. Choi I et al (2011) Visualization of lymphatic vessels by Prox1-promoter directed GFP reporter in a bacterial artificial chromosome-based transgenic mouse. Blood 117(1):362–365
34. Wang X et al (1997) Transgenic studies with a keratin promoter-driven growth hormone transgene: prospects for gene therapy. Proc Natl Acad Sci U S A 94(1):219–226
35. Barlic J, Murphy PM (2007) Chemokine regulation of atherosclerosis. J Leukoc Biol 82(2):226–236
36. Bozic CR et al (1994) The murine interleukin 8 type B receptor homologue and its ligands. Expression and biological characterization. J Biol Chem 269(47):29355–29358
37. Starckx S et al (2002) Recombinant mouse granulocyte chemotactic protein-2: production in bacteria, characterization, and systemic effects on leukocytes. J Interferon Cytokine Res 22(9):965–974
38. Waugh DJ, Wilson C (2008) The interleukin-8 pathway in cancer. Clin Cancer Res 14(21):6735–6741
39. Kunstfeld R et al (2004) Induction of cutaneous delayed-type hypersensitivity reactions in VEGF-A transgenic mice results in chronic skin inflammation associated with persistent lymphatic hyperplasia. Blood 104(4):1048–1057
40. Rutkowski JM et al (2006) Secondary lymphedema in the mouse tail: lymphatic hyperplasia, VEGF-C upregulation, and the protective role of MMP-9. Microvasc Res 72(3):161–171
41. Petrova TV et al (2002) Lymphatic endothelial reprogramming of vascular endothelial cells by the Prox-1 homeobox transcription factor. EMBO J 21(17):4593–4599
42. Hirakawa S et al (2003) Identification of vascular lineage-specific genes by transcriptional profiling of isolated blood vascular and lymphatic endothelial cells. Am J Pathol 162(2):575–586
43. Hong YK et al (2002) Prox1 is a master control gene in the program specifying lymphatic endothelial cell fate. Dev Dyn 225(3):351–357
44. Mu H et al (2012) Lysophosphatidic Acid induces lymphangiogenesis and IL-8 production in vitro in human lymphatic endothelial cells. Am J Pathol 180(5):2170–2181
45. Wigle JT et al (1999) Prox1 function is crucial for mouse lens-fibre elongation. Nat Genet 21(3):318–322
46. Dyer MA (2003) Regulation of proliferation, cell fate specification and differentiation by the homeodomain proteins Prox1, Six3, and Chx10 in the developing retina. Cell Cycle 2(4):350–357
47. Dyer MA et al (2003) Prox1 function controls progenitor cell proliferation and horizontal cell genesis in the mammalian retina. Nat Genet 34(1):53–58
48. Pan MR et al (2009) Sumoylation of Prox1 controls its ability to induce VEGFR3 expression and lymphatic phenotypes in endothelial cells. J Cell Sci 122(Pt 18):3358–3364
49. Kang J et al (2010) An exquisite cross-control mechanism among endothelial cell fate regulators directs the plasticity and heterogeneity of lymphatic endothelial cells. Blood 116(1):140–150
50. Nelson JD, Denisenko O, Bomsztyk K (2006) Protocol for the fast chromatin immunoprecipitation (ChIP) method. Nat Protoc 1(1):179–185
51. Zhang H et al (2011) Spontaneous lymphatic vessel formation and regression in the murine cornea. Invest Ophthalmol Vis Sci 52(1):334–338
52. Bos FL et al (2011) CCBE1 is essential for mammalian lymphatic vascular development and enhances the lymphangiogenic effect of vascular endothelial growth factor-C in vivo. Circ Res 109(5):486–491
53. Cao R et al (2011) Mouse corneal lymphangiogenesis model. Nat Protoc 6(6):817–826
54. Caunt M et al (2008) Blocking neuropilin-2 function inhibits tumor cell metastasis. Cancer Cell 13(4):331–342
55. Kubo H et al (2002) Blockade of vascular endothelial growth factor receptor-3 signaling inhibits fibroblast growth factor-2-induced lymphangiogenesis in mouse cornea. Proc Natl Acad Sci USA 99(13):8868–8873
56. Ecoiffier T, Yuen D, Chen L (2010) Differential distribution of blood and lymphatic vessels in the murine cornea. Invest Ophthalmol Vis Sci 51(5):2436–2440
57. Vassar R, Rosenberg M, Ross S, Tyner A, Fuchs E (1989) Tissue-specific and differentiation-specific expression of a human K14 keratin gene in transgenic mice. Proc Natl Acad Sci USA 86(5):1563–1567